BIOCHEMISTRY
including biophysical chemistry & molecular biology

Article

pubs.acs.org/biochemistry

Catalysis-Based Inhibitors of the Calcium Signaling Function of CD38

Anna Ka Yee Kwong,[†] Zhe Chen,[‡] HongMin Zhang,[†] Fung Ping Leung,[†] Connie Mo Ching Lam,[†] Kai Yiu Ting,[†] Liangren Zhang,[‡] Quan Hao,[†] Li-He Zhang,*[,‡] and Hon Cheung Lee*[,†]

[†]Department of Physiology, 4/F Lab Block, Faculty of Medicine Building, 21 Sassoon Road, University of Hong Kong, Hong Kong

[‡]State Key Laboratory of Natural and Biomimetic Drugs, School of Pharmaceutical Sciences, Peking University, Beijing 100191, China

ABSTRACT: CD38 is a signaling enzyme responsible for catalyzing the synthesis of cyclic ADP ribose (cADPR) and nicotinic acid adenine dinucleotide phosphate; both are universal Ca^{2+} messenger molecules. Ablation of the CD38 gene in mice causes multiple physiological defects, including impaired oxytocin release, that result in altered social behavior. A series of catalysis-based inhibitors of CD38 were designed and synthesized, starting with arabinosyl-2′-fluoro-2′-deoxynicotinamide mononucleotide. Structure−function relationships were analyzed to assess the structural determinants important for inhibiting the NADase activity of CD38. X-ray crystallography was used to reveal the covalent intermediates that were formed with the catalytic residue, Glu226. Metabolically stable analogues that were resistant to inactivation by phosphatase and esterase were synthesized and shown to be effective in inhibiting intracellular cADPR production in human HL-60 cells during induction of differentiation by retinoic acid. The inhibition was species-independent, and the analogues were similarly effective in blocking the cyclization reaction of CD38 in rat ventricular tissue extracts, as well as inhibiting the α-agonist-induced constriction in rat mesentery arteries. These compounds thus represent the first generally applicable and catalysis-based inhibitors of the Ca^{2+} signaling function of CD38.

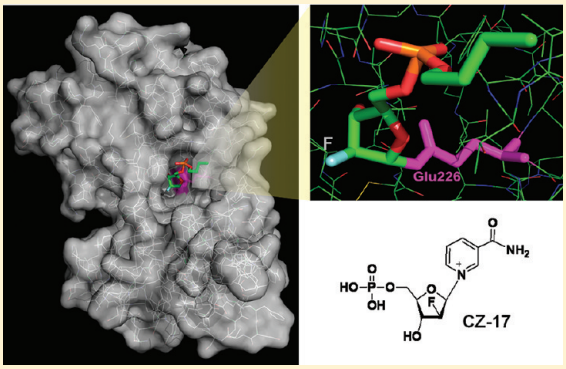

CD38 was first identified in lymphocytes by antibody typing[1,2] but has since been established to be an enzyme ubiquitously expressed in virtually all mammalian tissues (reviewed in refs 3 and 4). It has now been established that it is a signaling enzyme responsible for catalyzing the synthesis of two Ca^{2+} messengers, cyclic ADP ribose (cADPR) from NAD[5−7] and nicotinic acid adenine dinucleotide phosphate (NAADP) from NADP.[8,9] Both messenger molecules have been shown to regulate a wide range of physiological functions as diverse as abscisic acid signaling in plants[10] and sponges[11] and insulin secretion in mammalian β-cells[12−14] (reviewed in refs 15 and 16). The catalytic mechanism of how CD38 can catalyze the multiple reactions that lead to the synthesis of the two structurally and functional distinct messenger molecules has been well-characterized by crystallography and site-directed mutagenesis.[17−20] Recently, the multiple steps involved in cyclizing an NAD analogue to produce the cyclic product have been visualized by crystallography.[21,22]

Gene knockout studies have established that CD38 plays a critical role in a wide range of physiological functions from insulin secretion[23] and susceptibility to bacterial infection[24] to social behavior of mice through modulating neuronal oxytocin secretion.[25] It is thus of great interest to develop specific and generally applicable inhibitors of CD38. Among various inhibitors of CD38 that have been described, arabinosyl-2′-fluoro-2′-deoxynicotinamide mononucleotide (ara-2′F-NMN) is one of the more potent, with a half-maximal inhibitory concentration in the nanomolar range. Its inhibition is catalysis-dependent and forms a covalent intermediate with the catalytic residue of CD38.[26−28] However, the phosphate group of ara-2′F-NMN, critical for the inhibitory effect, is susceptible to hydrolysis by phosphatases that are prevalent in cells. In this study, ara-2′F-NMN is used as the starting compound to develop a series of metabolically stable inhibitors that can be used to block endogenous CD38 activity in cells and tissues.

MATERIALS AND METHODS

Recombinant CD38 Production. A yeast expression system, including the pPICZαA expression vector and *Pichia pastoris* yeast (Invitrogen), was used to prepare the recombinant CD38 as reported previously.[17,20]

Enzymatic Assays. The inhibition of the NAD glycohydrolase (NADase) reaction of CD38 by the CZ compounds was time-dependent, and the effect leveled off in ∼2 h (inset of Figure 1). As described in Results and Discussion, the inhibition was due to a covalent modification of CD38. The time dependency was thus a combination of the binding of the inhibitor to CD38 and it reacting covalently with it. It is,

Received: September 27, 2011
Revised: November 28, 2011
Published: December 5, 2011

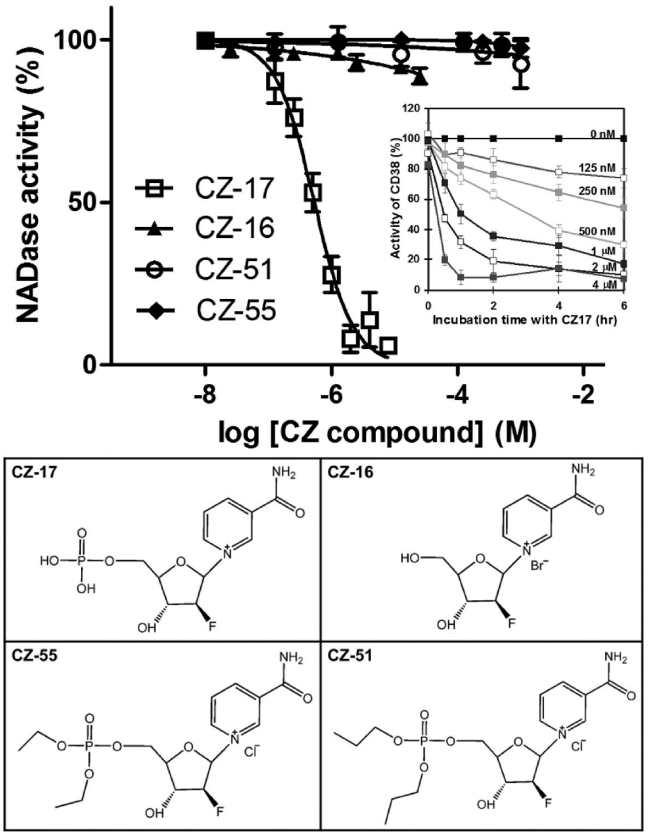

Figure 1. Importance of the phosphate group of ara-2′F-NMN for its inhibition of the NADase activity of CD38. Recombinant human CD38 was incubated with various concentrations of the analogues of ara-2′F-NMN (CZ-17) for 2 h, and its NADase activity was then measured as described in the text. The inset shows the time course of inhibition of CD38 by CZ-17. CD38 was incubated with CZ-17 for the times indicated. Reactions were started via the addition of 2 μM NAD to the CD38/inhibitor mixture and stopped with 300 mM HCl. The remaining NADase activity was determined. Data are expressed as the percent of control without CZ-17.

therefore, not appropriate to compare the effectiveness of various inhibitors using the conventional IC_{50} values. Instead, we compared the concentration of each inhibitor needed to produce half-maximal inhibition of the CD38 activity after incubation for 2 h.

The recombinant CD38 (0.3 ng) was mixed with different concentrations of the compounds in the presence of bovine serum albumin (1 μg) in a 16 μL reaction mixture and incubated in the dark for 2 h at room temperature. For measuring the inhibition of the NADase activity of CD38 by the CZ compounds, NAD was added to the mixture to a final concentration of 2 μM to start the reaction. Aliquots (4 μL) of the reaction mixture were taken at 0, 4, 8, or 12 min via addition of 4 μL of 0.6 M HCl, followed by neutralization with 8 μL of 0.5 M phosphate buffer (pH 8). The subsequent cycling reaction was conducted in 96-well plates with 16 μL of the sample mixed with 100 μL of the reagent containing 2% ethanol, 100 μg/mL alcohol dehydrogenase, 20 μM resazurin, 11 μg/mL diaphorase, 10 μM flavin mononucleotide, and 100 mM sodium phosphate (pH 7). The dilution greatly reduced the inhibitor concentration in the cycling assay. Using NAD standards, we verified that the inhibitors have little or no effect on the cycling assay under this condition. The cycling reaction was allowed to proceed for 10 min, and the rate of increase in resorufin fluorescence (with excitation at 544 nm and emission at 590 nm) was measured using the Infinite M200 fluorescence plate reader (TECAN). The relative NAD content was measured from the slopes of the fluorescent increase, and the NAD glycohydrolase activity was calculated from the decrease in the NAD content 0, 4, 8, and 12 min after the start of the reaction.

The cyclization reaction of CD38 was measured using nicotinamide guanine dinucleotide (NGD) as a substrate, which is cyclized to a fluorescent cyclic GDP ribose product described previously.[29] Rat left ventricles were homogenized in ice-cold 20 mM HEPES buffer with 1 mM EDTA and 0.1 mM phenylmethanesulfonyl fluoride. The homogenates were then centrifuged at 6000*g* for 5 min. Supernatant samples (500 μg protein each) were preincubated with different concentrations of the inhibitors for 1 h and added to a 0.12 mL reaction mixture, containing 50 mM Tris buffer (pH. 7.5) and 100 μM NGD. The production of the fluorescent product, cGDPR, was measured fluorimetically (excitation wavelength of 300 nm and emission wavelength of 410 nm) using the Infinite M200 fluorescence plate reader (TECAN). Rates of cGDPR production were determined from the slopes of the fluorescence increase.

Chemical Synthesis. Details of the chemical synthesis will be reported in a separate study.[49] Briefly, CZ-16 was obtained by coupling 3,5-di-*O*-benzoyl-2-deoxy-2-fluoro-α-D-arabinofuranose bromide[30] with nicotinamide at room temperature followed by deprotection. Phosphorylation of CZ-16 was performed by using a $POCl_3/PO(OCH_3)_3$ mixture[31] to produce CZ-17 (ara-F-NMN) or a $PSCl_3/PO(OCH_3)_3$ mixture to produce CZ-48. Esterification of CZ-17 was performed by treating it with an appropriate alcohol in a one-pot reaction to yield CZ-27, CZ-28, CZ-45, CZ-46, CZ-51, CZ-53, CZ-55, and CZ-57. CZ-30 and CZ-32 were obtained by a procedure similar to that used to prepare CZ-17, using 3,5-di-*O*-benzoyl-2-deoxy-2-chloro-α-D-arabinofuranose bromide and 3,5-di-*O*-benzoyl-2-deoxy-2-azido-α-D-arabinofuranose bromide, respectively. CZ-24 and CZ-50 were synthesized by coupling of 1,2-di-*O*-acetyl-5-*O*-benzoyl-3-deoxy-3-fluoro-D-xylofuranose[32] and 1-*O*-acetyl-3,5-di-*O*-benzoyl-2-deoxy-2-fluoro-D-ribose,[33] respectively, with nicotinamide in the presence of TMSOTf, followed by deprotection and phosphorylation. CZ-50 was an anomeric mixture that was separated to give CZ-50a (α-isomer) and CZ-50b (β-isomer). All products were purified by high-performance liquid chromatography and the chemical structures verified by nuclear magnetic resonance and HRMS.

Measurement of Intracellular cADPR Contents. HL-60 cells (4×10^5 cells/sample) were induced to differentiate with retinoic acid (1 μM) and treated with 0, 5, 10, and 20 μM CZ inhibitors for 3 days at 37 °C. Cells were then washed twice with phosphate-buffered saline, and cADPR was extracted from the cells with cold 0.6 M perchloric acid (PCA). The acid was removed by extraction with a 3:1 solution of chloroform and tri-*n*-octylamine. The neutral extracts were supplemented with Tris base to give a final pH of 8. The extracts were then treated with 0.44 unit/mL nucleotide pyrophosphatase and 2 mM $MgCl_2$ for 15−18 h at 37 °C to remove interfering nucleotides such as NAD, without degrading cADPR. After 15−18 h, the enzymes were removed by filtration through Immobilon-P filters (Millipore). The cADPR contents in the samples were then measured using the cycling assay as described previously.[34]

Vascular Preparations. Male Sprague-Dawley rats weighing 250−300 g were supplied from the Laboratory Animal Unit

Table 1. Data Collection and Refinement Statistics for Molecular Replacement[a]

	CZ-27	CZ-46	CZ-48	CZ-50b
		Data Collection		
space group	*P*1	*P*1	*P*1	*P*1
cell dimensions				
a, *b*, *c* (Å)	41.87, 53.66, 63.56	41.88, 53.51, 63.91	41.91, 50.85, 68.62	41.82, 53.63, 63.54
α, *β*, *γ* (deg)	109.56, 90.95, 94.73	109.33, 90.53, 94.83	68.62, 65.21, 83.60	109.72, 91.19, 94.81
resolution (Å)	50−1.65 (1.71−1.65)	50−1.91 (1.98−1.91)	50−2.05 (2.12−2.05)	50−1.95 (2.02−1.95)
R_{sym} or R_{merge}	0.071(0.399)	0.095(0.541)	0.069(0.384)	0.090(0.339)
$I/\sigma I$	19.4(3.9)	15.3(1.5)	23.4(3.5)	18.7(4.0)
completeness (%)	95.9(95.5)	94.9(86.8)	97.9(96.8)	97.7(96.6)
redundancy	3.9(4.0)	3.1(2.5)	3.5(3.4)	3.7(3.7)
		Refinement		
resolution (Å)	50−1.65	50−2.10	50−2.04	50−1.94
no. of reflections	56509	27735	29932	35482
R_{work}/R_{free}	0.180/0.209	0.216/0.275	0.183/0.227	0.173/0.209
no. of atoms				
protein	4099	4071	4089	4086
compound	34	42	26	26
water	368	198	237	266
B factor				
protein	15.2	10.9	13.8	13.7
compound	32.9	45.6	42.6	34.4
water	26.2	14.8	21.7	22.9
root-mean-square deviation				
bond lengths (Å)	0.009	0.011	0.008	0.010
bond angles (deg)	1.282	1.289	1.088	1.185

[a]Values in parentheses are for the highest-resolution shell.

of the University of Hong Kong. Rats were anesthetized with pentobarbitone sodium (50 mg/kg, by intraperitoneal injection) and then sacrificed by cervical dislocation. All experiments performed in this study were approved by the Committee on the Use of Live Animals in Teaching and Research of the University of Hong Kong. The ileum and associated mesentery were quickly dissected and immersed in ice-cold (4 °C) Krebs solution bubbled with a 95% O_2/5% CO_2 gas mixture. The fourth-order mesenteric artery (~2−3 mm long) with an outer diameter of 250−350 μm was carefully dissected free of the surrounding adipose tissue under a dissection microscope. The artery was cut into short ring segments with each suspended by two stainless steel wires in the 5 mL chamber of a Multi Myograph System (Danish Myo Technology, Aarhus, Denmark) with Krebs solution constantly bubbled with a 95% O_2/5% CO_2 gas mixture and maintained at 37 °C. Changes in vessel diameter were then measured. The rings were placed under an optimal basal tone of 2 mN, determined from previous length−tension experiments. Changes in isometric tension were measured with a force transducer and stored on labchart software for later data analysis. Twenty minutes after being mounted in organ baths, the rings were first contracted with 1 μM phenylephrine (Phe) to test the contractility and then relaxed with 1 μM acetylcholine. They were rinsed several times until baseline tone was restored. The rings were thereafter allowed to equilibrate for 60 min. Baseline tone was readjusted to 2 mN when necessary. Each set of experiments was performed on rings prepared from different rats.

Vascular Tension Measurements. In this set of experiments, relaxation of (3 μM) Phe-contracted endothelium-intact rings was induced by CZ-48 (30−300 μM), CZ-24 (30−300 μM), or nicotinamide (0.01−6 mM). All chemicals were dissolved in milliQ water (MQ).

The relaxant effects of the vasodilators were expressed as 100 minus the percent reduction from the Phe-induced contractile response. Nonlinear regression curve fitting was performed on individual cumulative concentration−response curves (GraphPad, version 5.0). The half-maximal effective concentration values were calculated as negative log molar values of dilator that induced 50% of the maximal relaxation. All data are means ± SEM. Statistical significance was determined by a two-tailed Student's *t* test or one-way ANOVA followed by the Newman−Keuls test when more than two treatments were compared. A *P* value of <0.05 was defined as being significant.

Crystallization, Data Collection, and Structure Refinement. Crystals of CD38 in complex with compounds were obtained by cocrystallization using the hanging drop vapor diffusion method. CD38 protein in 20 mM HEPES buffer was mixed with the CZ compounds to give a final CD38 concentration of 10 mg/mL and a final compound concentration of 5 mM. The mixture was then added to an equal volume of the reservoir buffer [0.1 M sodium acetate (pH 4.0), 0.2 M ammonium acetate, 3% 2-propanol, and 15% PEG 10000] for cocrystallization. The crystals were soaked in cryo buffer in 0.1 M sodium acetate (pH 4.0), 20% glycerol, and 20% PEG 10000. They were harvested and flash-frozen in liquid nitrogen. The diffraction data were collected at 100 K at BL17U at the Shanghai Synchrotron Radiation Facility and processed with HKL2000.[35] Molecular replacement was performed using Phaser[36] from CCP4[37] with the wild-type human CD38 [Protein Data Bank (PDB) entry 1YH3] as the searching model. The model was refined with Refmac[38] and then cycled with rebuilding in Coot.[39] The ara-2′F product was built into positive difference electron density maps after a few

restrained refinement runs of the protein models with the stereochemical restraints generated using PRODRG.[40] TLS refinement[41] was incorporated into the later stages of the refinement process. Solvents were added automatically in Coot and then manually inspected and modified. The final model was analyzed with MolProbity.[42] Data collection and model refinement statistics are summarized in Table 1. The coordinates and structure factors of wild-type CD38 in complex with hydrolyzed compounds CZ-27, CZ-46, CZ-48, and CZ-50b were deposited in the PDB as entries 3ROK, 3ROQ, 3ROM, and 3ROP, respectively.

RESULTS AND DISCUSSION

Ara-2′F-NMN (CZ-17) inhibited the NADase reaction of CD38 in a concentration- and time-dependent manner, with a half-maximal inhibition concentration of ~0.5 μM (Figure 1). We have previously shown by X-ray crystallography that CZ-17 forms a covalent intermediate with CD38.[27] The nicotinamide group is cleaved, and the anomeric carbon is covalently linked to the catalytic residue, Glu226.

Structure−Function Relationship of the Analogues of Ara-2′F-NMN. To elucidate the structural determinants of Ara-2′F-NMN (CZ-17) for its inhibitory effect, we synthesized a series of analogues. As shown in Figure 1, the negative charge on the phosphate was critical for the inhibition. Eliminating the charges by attaching alkyl groups to the phosphate or by deleting the group altogether rendered CZ-17 inactive in inhibiting the NADase reaction.

Attaching a monoalkyl group to the phosphate, thus preserving a negative charge on the group, preserved its inhibitory effect, as shown in Figure 2. The length of the alkyl

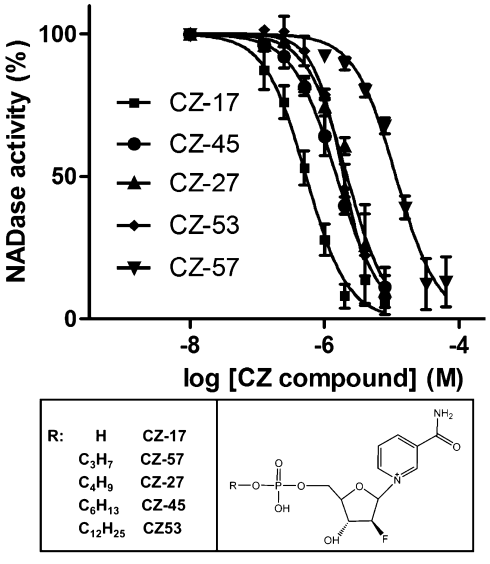

Figure 2. Effects of attaching alkyl chains of various lengths to the phosphate of ara-2′F-NMN on its inhibitory ability. Recombinant human CD38 was incubated with various concentrations of the analogues of ara-2′F-NMN (CZ-17) for 2 h, and its NADase activity was then measured as described in the text.

chain was important. The analogue with a short three-carbon chain (CZ-57) was least inhibitory, requiring a concentration of 11 μM to produce half-maximal inhibition, 22 times higher than that of CZ-17. Analogues (CZ-27, CZ-45, and CZ-53) with chains containing four or more carbons were much more inhibitory; all required a concentration of ~2 μM to produce half-maximal inhibition, making them 10 times more effective than CZ-57.

The orientation of the fluorine at position 2′ has very little effect on the inhibition of the NADase (Figure 3). CZ-50b,

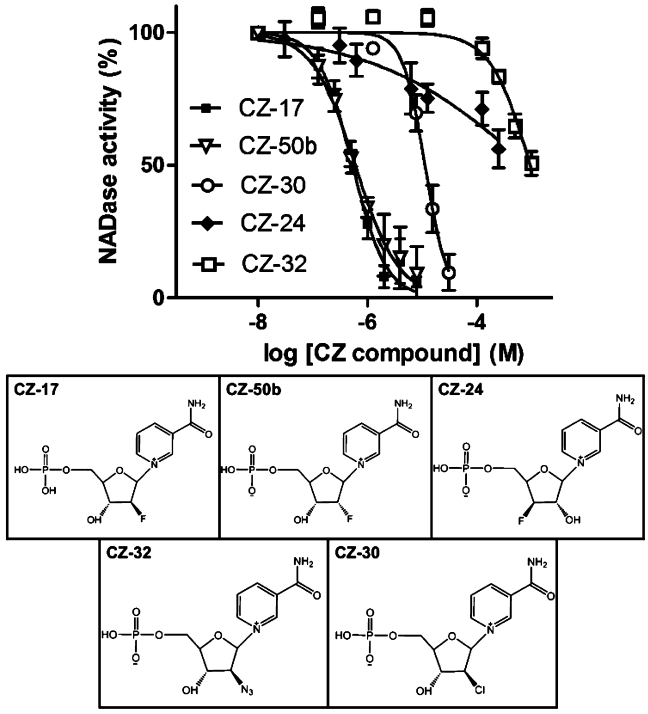

Figure 3. Role of the fluorine on the ribose of ara-2′F-NMN in its inhibitory ability. Recombinant human CD38 was incubated with various concentrations of the analogues of ara-2′F-NMN (CZ-17) for 2 h, and its NADase activity was then measured as described in the text.

whose fluorine is in the *syn* position (ribose form) with respect to the OH group at position 3′, had an effectiveness similar to that of CZ-17 with the fluorine in the *anti* orientation (arabinose form), requiring a concentration ~0.6 μM to produce half-maximal inhibition. However, as shown in Figure 3, switching the fluorine to position 3′ as in CZ-24 dramatically increased the half-maximal effective concentration by more than 500 times to >0.25 mM. Fluorine is a strong electron-withdrawing group. Its presence at position 2′ should promote the cleavage of the nicotinamide ring and the formation of the covalent intermediate. Consistently, moving it to position 3′ increases its distance from the anomeric carbon and slows formation of the intermediate, and hence the inhibition. Changing the fluorine to chlorine (CZ-30) increased the effective concentration to 11 μM, which was further increased to >1 mM with an N_3 substituent (CZ-32). This correlates with the chloro and azido groups having much weaker electron withdrawing ability than the fluoro group.

Figure 4 shows that changing one of the oxygens of the phosphate to sulfur (CZ-48) had a minimal effect. The concentration of 2 μM required to produce half-maximal inhibition was higher than that of CZ-17 but was comparable to the effect of attaching an alkyl group to the phosphate (cf. Figure 2). The slight reduction of the effectiveness of the sulfur analogue can thus be attributed to the charge reduction of the phosphate that was the same as that of the phosphate ester

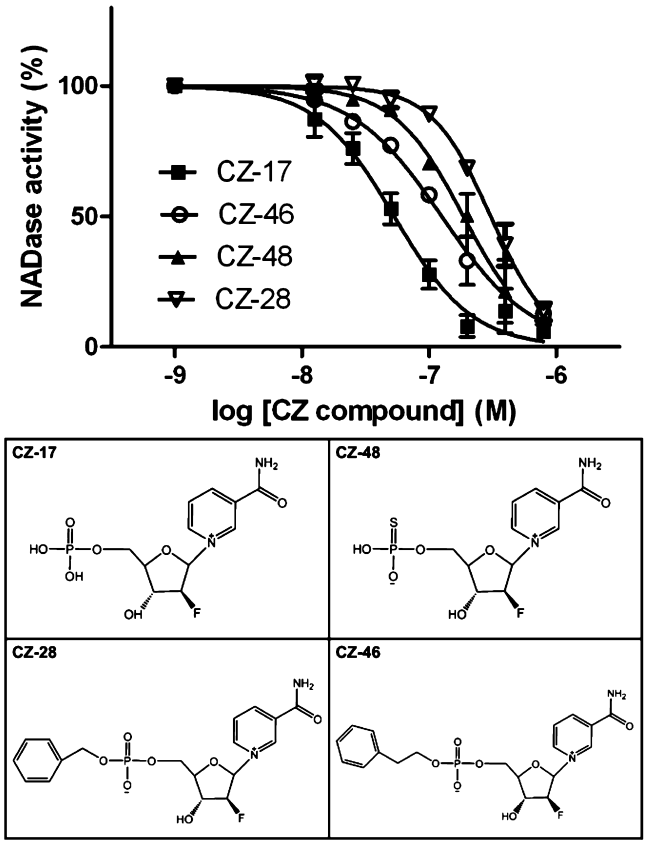

Figure 4. Effects of modifying the phosphate or the nicotinamide groups of ara-2′F-NMN on its inhibitory ability. Recombinant human CD38 was incubated with various concentrations of the analogues of ara-2′F-NMN (CZ-17) for 2 h, and its NADase activity was then measured as described in the text.

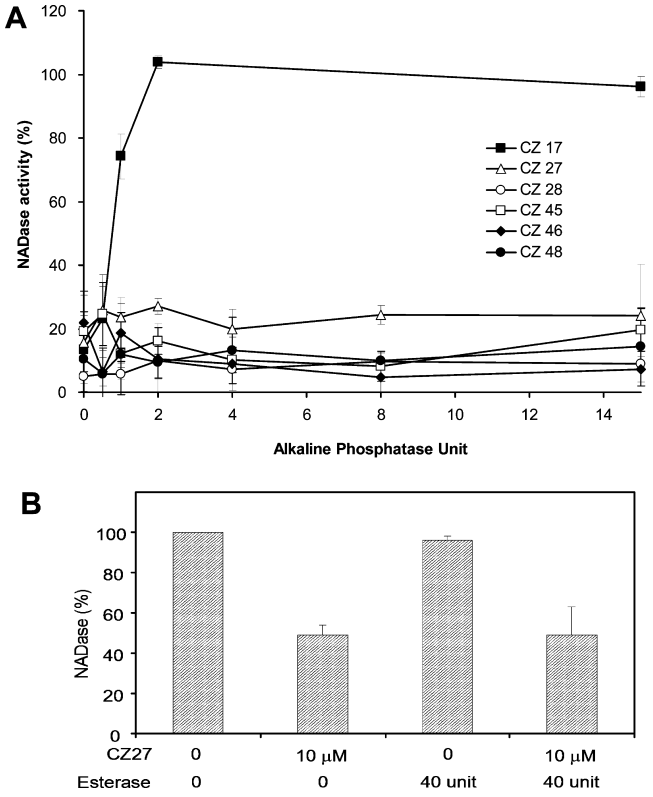

Figure 5. Stability of the analogues of ara-2′F-NMN against alkaline phosphatase and esterase. (A) Various analogues of ara-2′F-NMN were incubated with the indicated concentrations of alkaline phosphatase for 2 h at 37 °C. After removal of the phosphatase using Immobilon-P filters, the analogues were tested for the ability to inhibit the NADase activity of CD38. The concentration of all the CZ compounds tested was 20 μM, except that of CZ-48, which was tested at 10 μM. (B) The procedure was the same as that used for panel A, except that CZ-27 was incubated with the esterase for 2 h at room temperature.

analogues. Attaching a bulkier aromatic group, such as a benzene ring, to the phosphate also has a minimal effect. For CZ-28 and CZ-46, concentrations of 3 and 1.3 μM, respectively, were required to produce half-maximal inhibition. The structure−function relationship described above indicates that the catalysis-based inhibitors for CD38 are highly specific. Even a slight change in the structure of the compounds can entirely eliminate the inhibitory effect.

Stability of the Inhibitors. As described above, the phosphate group is critical for the inhibitory effect but susceptible to hydrolysis by phosphatases that are prevalent in cells. Ara-2′F-NMN is thus unlikely to be useful as a generally applicable inhibitor for CD38 in cells and tissues. Indeed, as shown in Figure 5A, treatment of CZ-17 with alkaline phosphatase effectively eliminated its inhibitory effect on CD38. However, the attachment of a single hydrocarbon substituent to phosphate, as in CZ-27, CZ-28, CZ-45, and CZ-46, made it stable against alkaline phosphatase, as was the sulfur analogue, CZ-48. These compounds, although slightly less effective than CZ-17, should be more useful as inhibitors of CD38 in cells and tissues. The reduction in charge on the phosphate and the increased hydrophobicity due to the hydrocarbon substituent should also make these compounds more permeant to cells and tissues.

Importantly, the ester linkage between the hydrocarbon substituent and the phosphate was found to be stable against esterase activity that is also prevalent in cells and tissues. This was tested using CZ-27 as shown in Figure 5B. It retained its inhibitory effect on CD38 even after prolonged treatment with high concentrations of esterase. The control shows that the esterase used was fully effective in hydrolyzing the ester bonds of the acetoxymethoxy (AM) groups of fluo 3-AM and converting it to fluo 3.

Crystal Structures of the Covalent Intermediates. We selected CZ-27 for structural analysis because it is most suitable for use in cells and tissues, as described above. The crystal structure of CZ-27 in a complex with CD38 is shown in Figure 6. There were two molecules in each asymmetric unit, and each had a covalent intermediate of CZ-27 (rendered as sticks) bound at the middle of the molecule (Figure 6A).

The interactions between the bound intermediate and the active residues are shown in stereoview in Figure 6B. The linkage between the carboxyl oxygen of Glu226 and the anomeric carbon of the ribose of CZ-27 was 1.4 Å in length, consistent with a covalent bond. The nicotinamide ring of CZ-27 was cleaved and released. The fluorine at position 2′ of the ribose of CZ-27 was in the *anti* orientation with respect to the 3′-hydroxyl, which formed hydrogen bonds (cyan dash) with both the amide nitrogen of Trp125 and a bound water molecule.

Likewise, the phosphate was well-positioned through hydrogen bonding with the amide nitrogens of Phe222 and Arg127, as well as with the hydroxyl group of Ser126. These interactions

dx.doi.org/10.1021/bi201509f | *Biochemistry* 2012, 51, 555−564

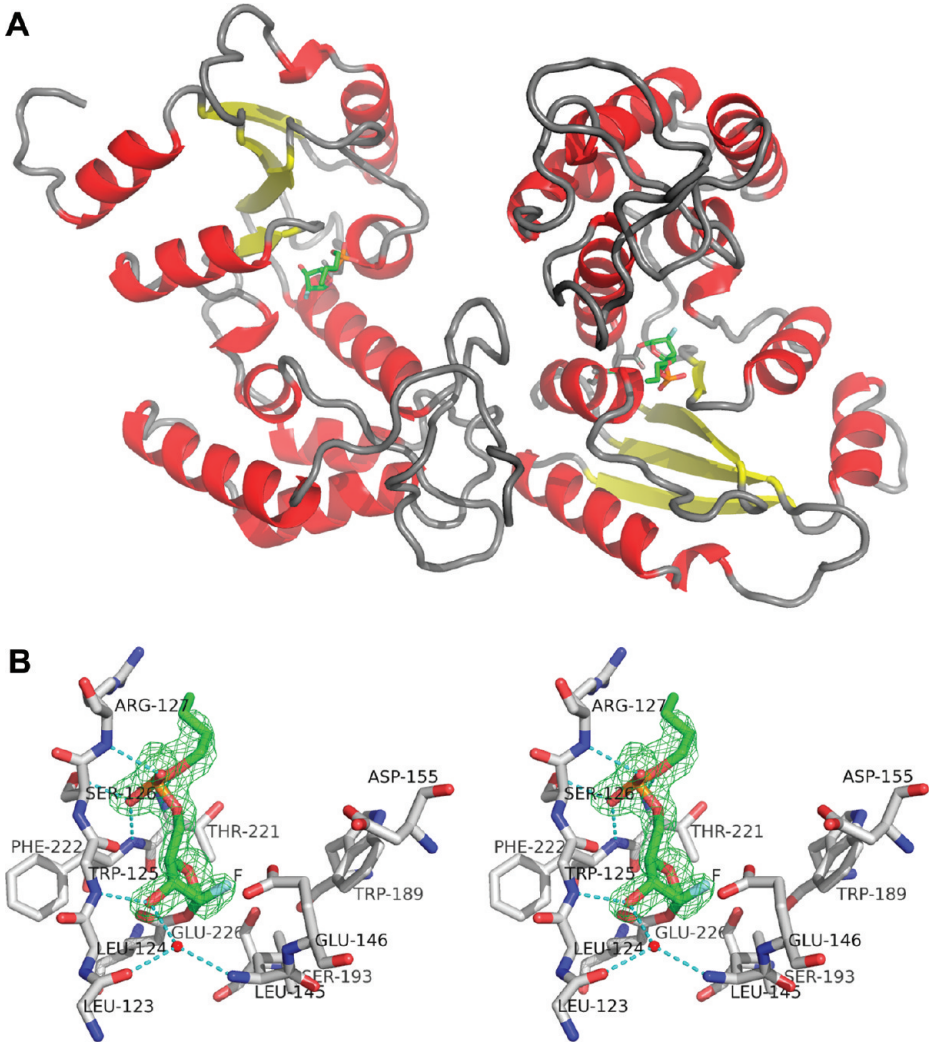

Figure 6. Structure of human CD38 in a complex with compound CZ-27. (A) Ribbon display of the two molecules of CD38 in a crystal asymmetric unit. Each CD38 molecule has a catalysis intermediate covalently bound near the middle of the protein. The intermediates are rendered as sticks. Phosphorus is colored orange, oxygen red, carbon green, and fluorine cyan. The secondary structures of CD38 are shown with helices colored red, β-sheets yellow, and coils gray. (B) Stereoview of the covalent intermediate CZ-27 at the active site. The carbons of residues at the active site are colored gray and nitrogens blue. The color coding for the covalent intermediate is the same as that in panel A. Cyan dashes represent hydrogen bonds. The $F_o - F_c$ map for the covalent intermediate is shown as green mesh at 3.0σ.

should contribute to the affinity of CZ-27 for the active site. The importance of the charges on the phosphate for the inhibitory effect of CZ-27 is thus clear. Elimination of the charges, as in CZ-51 and CZ-55 (cf. Figure 1), certainly would disrupt the hydrogen bonding and prohibit binding of CZ-27 to the active site.

Figure 7A shows the superposition of the two CD38 molecules in the asymmetric unit and focuses on the active site. The ribose units of the intermediates of both CD38 molecules superimposed very well. However, the two hydrocarbon chains (carbon colored transparent cyan and opaque white) attached to the phosphate had completely different conformations. Also, both were directed outward from the active site pocket. These structural features indicate the chain is flexible, and its length or bulkiness should not interfere with its function as an inhibitor, because it is mainly outside the active site. This is consistent with the functional results shown in Figures 2 and 4. This structural feature can be exploited to produce useful probes for CD38. For example, a fluorescent group can be attached to the end of a long hydrocarbon chain to produce a fluorescent probe for labeling CD38 in cells and tissues.

The crystal structures of the complexes of three other inhibitors, CZ-46, CZ-48, and CZ-50b, were also determined to assess the generality. All of them formed covalent intermediates with Glu226. Figure 7B shows the alignment of the two CZ-46 intermediates in the two CD38 molecules in the asymmetric unit. As opposed to CZ-27, the two benzene rings in the CZ-46 intermediates superimposed quite closely. Other than that, the structure of the intermediate was essentially identical to that of CZ-27.

The same was true for CZ-48 as shown in Figure 7C. The sulfur atom that replaced one of the oxygens of the phosphate, similar to the hydrocarbon chain in CZ-27 and the benzene ring in CZ-46, was also pointing outward from the active site. The structural similarity of all these three intermediates is consistent with the fact that they are similarly effective in inhibiting CD38 (Figures 2 and 4).

Figure 7D shows a similar surface view of the active site pocket with an intermediate of CZ-50b covalently linked to

dx.doi.org/10.1021/bi201509f | *Biochemistry* 2012, 51, 555–564

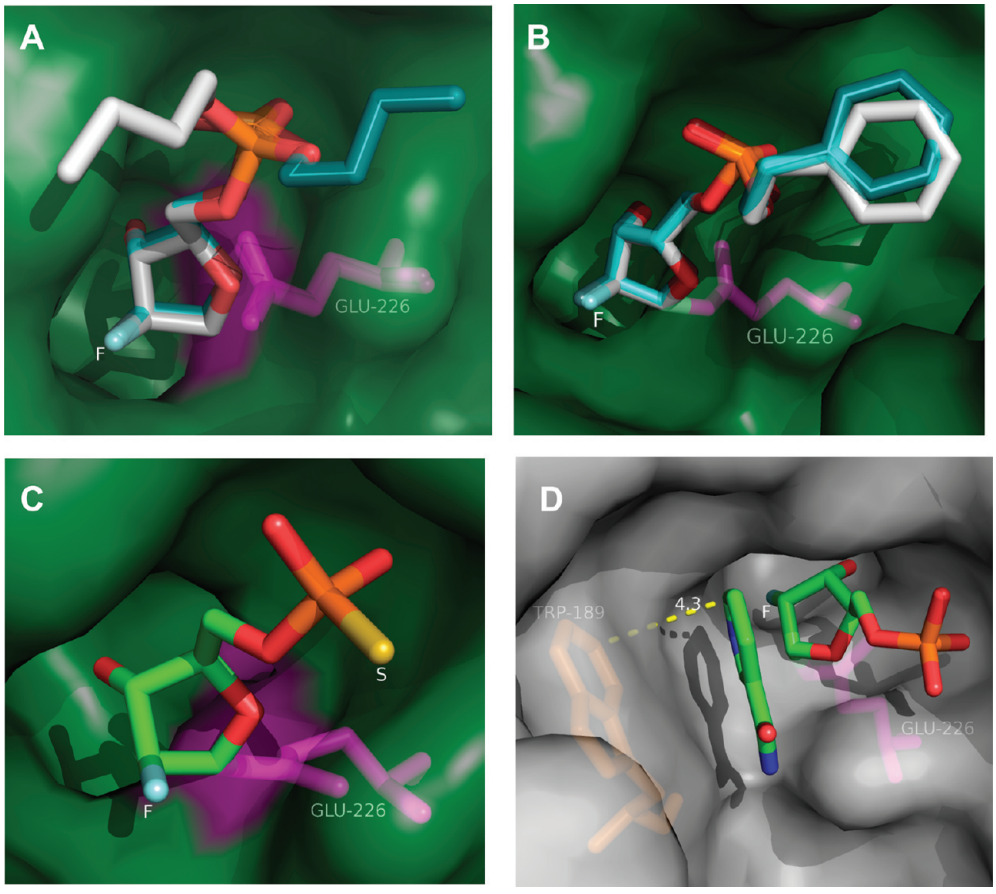

Figure 7. Structure at the active site of CD38. CD38 is shown as a surface with residue Glu226 shown as a magenta stick. The covalent intermediates at the active site are shown as stick models with oxygens colored red, phosphates orange, fluorines cyan, and sulfurs gold. (A) Superposition of the two CD38 molecules in the crystal asymmetric unit showing the differences between the two CZ-27 intermediates of the CD38−CZ-27 complex. The carbon atoms of the two CZ-27 intermediates are colored white and transparent cyan. (B) Similar superimposition of the intermediates of CZ-46. The color coding is the same as that in panel A. (C) Covalent intermediate of CZ-48 at the active site of CD38. The carbon atoms of CZ-48 are colored green. (D) Covalent intermediate of CZ-50b at the active site of CD38. The cleaved nicotinamide ring could also be seen in the refined structure and is shown as stick models stacking close to the side chain of residue Trp189 with a distance of 4.3 Å. The color coding for CZ-50b and nicotinamide is the same as in Figure 6.

Glu226. The fluorine can be seen to have a *syn* orientation with respect to the 3′-hydroxyl of the ribose, contrasting with the *anti* orientation in CZ-27 and confirming the chemical structure of the compound. Also present in the active site, in this case, is the cleaved nicotinamide ring, which stacked parallel to Trp189 at a distance of 4.3 Å, suggesting hydrophobic interaction.

Cellular Application. We have previously shown that induction of differentiation in human HL-60 cells by retinoic acid is accompanied by continuous and strong expression of CD38 as well as concomitant elevation of the cellular content of cADPR.[43] The differentiation takes ~3 days. The stability of the inhibitors as shown in Figure 5 makes it possible to apply them to this process. Figure 8 shows that CZ-27 was effective in inhibiting the increase in the cellular concentration of cADPR in a concentration-dependent manner. The half-maximal effective concentration was ~10 μM, similar to its effectiveness in inhibiting the NADase activity of CD38 (Figure 2). To demonstrate specificity, we also tested CZ-24, which required a concentration of >0.25 mM to produce half-maximal inhibition (Figure 3). Consistently, it did not have a notable effect on the cADPR content even at 20 μM. The inhibition of cADPR production in the cells was not complete, probably because of the continuous expression and turnover of CD38 associated with the differentiation process. Alternatively, the negatively charged CZ-27 might not have access to all CD38 in the cells, as it is known that CD38 is expressed as an ecto-enzyme on cell surfaces and in intracellular organelles.[43−45] The development of both impermeant and permeant inhibitors, as started in this study, can potentially be useful in dissecting the physiological functions of ecto-CD38 and intracellular CD38.

Tissue Application. It has previously been shown that cADPR is responsible for mediating α-adrenergic Ca^{2+} signaling in rat lacrimal acinar cells.[46] Similarly, ablation of CD38, the enzyme responsible for cADPR synthesis, results in impairment of the aortic contraction induced by α-adrenoceptor stimulation.[47] We therefore tested the effect of CZ-48 on the phenylephrine-induced contraction of rat arteries.

As described above, the inhibitory effects of the CZ compounds are catalysis-based and require specific interactions with the active site of CD38. Currently, only the structure of human CD38 has been determined, and how similar it is with that of rat CD38 is not known. We thus tested first if CZ-27 can inhibit rat CD38 activity. We used rat heart extracts and measured the cyclization activity of CD38 using NGD, which is cyclized to fluorescent cGDPR.[29] This reaction is specific for CD38 and suitable for use in tissue extracts because other NAD-utilizing enzymes do not catalyze cGDPR production. As shown in Figure 9A, CZ-27 inhibited cGDPR production in rat

dx.doi.org/10.1021/bi201509f | *Biochemistry* 2012, 51, 555−564

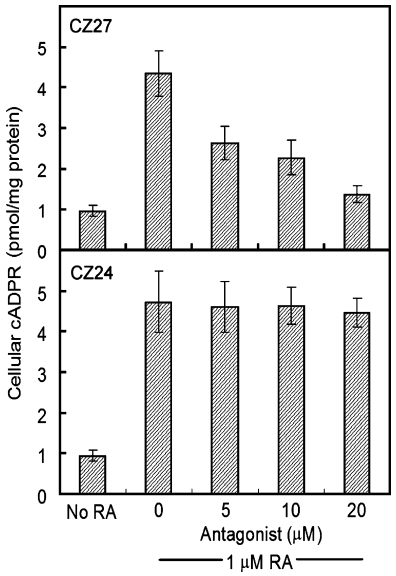

Figure 8. Inhibition of the production of intracellular cADPR. Human HL-60 cells were treated with retinoic acid (1 μM) to induce differentiation, with or without various concentrations of CZ-27 or CZ-24. After 3 days, the intracellular cADPR contents were measured as described in the text. The data are means ± SEM of three individual experiments.

heart extracts with a half-maximal effective concentration of <5 μM, similar to that needed for its inhibition of the NADase activity of human recombinant CD38. CZ-24 showed no inhibition, similar to that seen in human CD38. CZ-48 inhibited the cyclization reaction in rat heart tissue extracts also, but less effectively than CZ-27. In human CD38, both were similarly effective. This can be attributed to possible differences in the active sites. Nevertheless, the results suggest that the catalytic mechanism and structure of the active site of rat CD38 should be quite similar to those of human CD38 and that the CZ compounds can be applied to both species.

Figure 9B shows that, as expected, CZ-48 inhibited the Phe-induced contraction of rat mesentery arteries with a half-maximal effective concentration of ~30 μM, while the inactive analogue, CZ-24 (Figure 3), had little effect up to 300 μM. The vascular relaxing effects of CZ-48 were confirmed by nicotinamide, a known inhibitor of CD38[43,48] (Figure 9C). The half-maximal effective concentration of nicotinamide on inhibiting contraction was much higher, ~2.2 mM. It should be noted that nicotinamide is not actually an inhibitor of CD38; instead, at high concentrations, it reverses its NAD hydrolysis and cyclization reactions.[34]

In summary, this study provides evidence that the CZ compounds are generally applicable and reasonably specific inhibitors of CD38. These compounds have been tested in cells and vascular tissues. Both CZ-24 and CZ-48 are less charged and more hydrophobic than ara-F-NMN, and it is reasonable to expect them to be cell permeant and able to inhibit both ecto-CD38 and intracellular CD38. The mechanisms of their inhibitory effects have been elucidated by X-ray crystallography and structure−function analyses. These specific inhibitors have advantages over the gene knockout approach for assessing the physiological roles of CD38, because they are applied acutely, making the inhibition unlikely to be obscured by possible compensatory mechanisms that are commonly developed in knockout mice. Also, as shown in this study, the inhibitors are

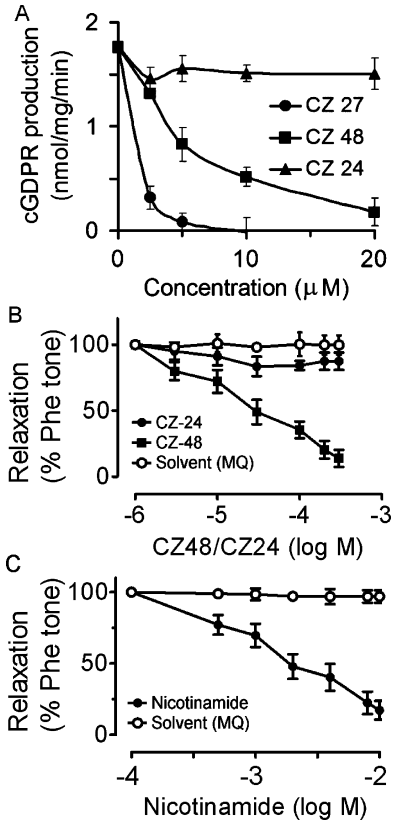

Figure 9. Inhibition of CD38 activity and α-agonist-induced vascular constriction. (A) The cyclization activity of CD38 in the extracts of rat heart was measured as the rate of production of cGDPR from NGD as a substrate as described in the text. (B) Isolated mesentery arterial ring preparations from rats were preconstricted with 3 μM phenylephrine. Sequential addition of increasing concentrations of CZ-48 induced progressive relaxation. Neither the inactive analogue, CZ-24, nor the solvent (MQ water) control produced similar vascular relaxation. Data are means ± SEM of five measurements, except with CZ-24, which were means ± SEM of three measurements. (C) Same as panel B, except nicotinamide was tested. Data are means ± SEM of five measurements.

species-independent, and thus, their applications are not limited to mice as gene ablation is. They should thus be valuable tools for dissecting the CD38/cADPR signaling pathway.

AUTHOR INFORMATION

Corresponding Author

*H.C.L.: e-mail, leehc@hku.hk; phone, 852-2819-9163; fax, 852-2817-1334. L.-H.Z.: e-mail, zdszlh@bjmu.edu.cn; phone and fax, 10-82801700.

Author Contributions

A.K.Y.K., Z.C., H.M.Z., and F.P.L. contributed equally to this work.

Funding

This work was supported by grants from the Hong Kong General Research Fund (RGC) (769107, 768408, 769309, and 770610 to H.C.L. and 765909 and 766510 to Q.H.), the National Natural Sciences Foundation of China/RGC Joint Research Scheme (NSFC/RGC Grant N_HKU 722/08 to H.C.L.), and a NSFC grant to L.-H.Z. (NSFC-RGC 20831160506 and NSFC 81172917).

■ ACKNOWLEDGMENTS

We are thankful for the technical help of Victor Wai Lung Chan and the staff at the Shanghai Synchrotron Radiation Facility.

■ ABBREVIATIONS

NAD, nicotinic acid dinucleotide; NADase, NAD glycohydrolase; cADPR, cyclic ADP ribose; ara-2′F-NMN, arabinosyl-2′-fluoro-2′-deoxynicotinamide mononucleotide; NGD, nicotinamide guanine dinucleotide; NAADP, nicotinic acid adenine dinucleotide phosphate; Phe, phenylephrine; MQ, milliQ water; PCA, perchloric acid; HEPES, *N*-(2-hydroxyethyl)-piperazine-*N*′-2-ethanesulfonic acid; Tris, tris(hydroxymethyl)-aminomethane; HRMS, high-resolution mass spectrometry; TMSOTf, trimethylsilyl triflate; SEM, standard error of the mean.

■ REFERENCES

(1) Reinherz, E. L., Kung, P. C., Goldstein, G., Levey, R. H., and Schlossman, S. F. (1980) Discrete stages of human intrathymic differentiation: Analysis of normal thymocytes and leukemic lymphoblasts of T-cell lineage. *Proc. Natl. Acad. Sci. U.S.A. 77*, 1588−1592.

(2) Jackson, D. G., and Bell, J. I. (1990) Isolation of a cDNA encoding the human CD38 (T10) molecule, a cell surface glycoprotein with an unusual discontinuous patern of expression during lymphocyte differentiation. *J. Immunol. 144*, 2811−2815.

(3) Lee, H. C. (2006) Structure and enzymatic functions of human CD38. *Mol. Med. 12*, 317−323.

(4) Lee, H. C., Graeff, R. M., and Walseth, T. F. (1997) ADP-ribosyl cyclase and CD38. Multi-functional enzymes in Ca^{2+} signaling. *Adv. Exp. Med. Biol. 419*, 411−419.

(5) Lee, H. C., Aarhus, R., and Levitt, D. (1994) The crystal structure of cyclic ADP-ribose. *Nat. Struct. Biol. 1*, 143−144.

(6) Lee, H. C., Walseth, T. F., Bratt, G. T., Hayes, R. N., and Clapper, D. L. (1989) Structural determination of a cyclic metabolite of NAD^+ with intracellular Ca^{2+}-mobilizing activity. *J. Biol. Chem. 264*, 1608−1615.

(7) Howard, M., Grimaldi, J. C., Bazan, J. F., Lund, F. E., Santos-Argumedo, L., Parkhouse, R. M., Walseth, T. F., and Lee, H. C. (1993) Formation and hydrolysis of cyclic ADP-ribose catalyzed by lymphocyte antigen CD38. *Science 262*, 1056−1059.

(8) Aarhus, R., Graeff, R. M., Dickey, D. M., Walseth, T. F., and Lee, H. C. (1995) ADP-ribosyl cyclase and CD38 catalyze the synthesis of a calcium-mobilizing metabolite from NADP. *J. Biol. Chem. 270*, 30327−30333.

(9) Lee, H. C., and Aarhus, R. (1995) A derivative of NADP mobilizes calcium stores insensitive to inositol trisphosphate and cyclic ADP-ribose. *J. Biol. Chem. 270*, 2152−2157.

(10) Wu, Y., Kuzma, J., Marechal, E., Graeff, R., Lee, H. C., Foster, R., and Chua, N. H. (1997) Abscisic acid signaling through cyclic ADP-ribose in plants. *Science 278*, 2126−2130.

(11) Zocchi, E., Carpaneto, A., Cerrano, C., Bavestrello, G., Giovine, M., Brozzone, S., Guida, L., Franco, L., and Usai, C. (2001) The temperature-signaling cascade in sponges involves a heat-gated cation channel, abscisic acid and cyclic ADP-ribose. *Proc. Natl. Acad. Sci. U.S.A. 98*, 14859−14864.

(12) Johnson, J. D., and Misler, S. (2002) Nicotinic acid-adenine dinucleotide phosphate-sensitive calcium stores initiate insulin signaling in human β cells. *Proc. Natl. Acad. Sci. U.S.A. 99*, 14566−14571.

(13) Kim, B.-J., Park, K.-H., Yim, C.-Y., Takasawa, S., Okamoto, H., Im, M.-J., and Kim, U.-H. (2008) Generation of NAADP and cADPR by glucagon-like peptide-1 evokes Ca^{2+} signal that is essential for insulin secretion in mouse pancreatic islets. *Diabetes 57*, 868−878.

(14) Takasawa, S., Nata, K., Yonekura, H., and Okamoto, H. (1993) Cyclic ADP-ribose in insulin secretion from pancreatic β cells. *Science 259*, 370−373.

(15) Lee, H. C. (2002) Cyclic ADP-ribose and NAADP. *Structures, Metabolism and Functions*, Kluwer Academic Publishers, Dordrecht, The Netherlands.

(16) Lee, H. C. (2004) Multiplicity of Ca^{2+} messengers and Ca^{2+} stores: A perspective from cyclic ADP-ribose and NAADP. *Curr. Mol. Med. 4*, 227−237.

(17) Liu, Q., Kriksunov, I. A., Graeff, R., Lee, H. C., and Hao, Q. (2007) Structural basis for formation and hydrolysis of calcium messenger cyclic ADP-ribose by human CD38. *J. Biol. Chem. 282*, 5853−5861.

(18) Liu, Q., Kriksunov, I. A., Graeff, R., Munshi, C., Lee, H. C., and Hao, Q. (2005) Crystal structure of human CD38 extracellular domain. *Structure 13*, 1331−1339.

(19) Liu, Q., Kriksunov, I. A., Graeff, R., Munshi, C., Lee, H. C., and Hao, Q. (2006) Structural basis for the mechanistic understanding of human CD38 controlled multiple catalysis. *J. Biol. Chem. 281*, 32861−32869.

(20) Munshi, C., Aarhus, R., Graeff, R., Walseth, T. F., Levitt, D., and Lee, H. C. (2000) Identification of the enzymatic active site of CD38 by site-directed mutagenesis. *J. Biol. Chem. 275*, 21566−21571.

(21) Graeff, R., Liu, Q., Kriksunov, I. A., Kotaka, M., Oppenheimer, N., Hao, Q., and Lee, H. C. (2009) Mechanism of cyclizing NAD to cyclic ADP-ribose by ADP-ribosyl cyclase and CD38. *J. Biol. Chem. 284*, 27629−27636.

(22) Zhang, H., Graeff, R., Chen, Z., Zhang, L., Lee, H., and Hao, Q. (2011) Dynamic Conformations of the CD38-mediated NAD cyclization captured in a single crystal. *J. Mol. Biol. 405*, 1070−1078.

(23) Kato, I., Yamamoto, Y., Fujimura, M., Noguchi, N., Takasawa, S., and Okamoto, H. (1999) CD38 disruption impairs glucose-induced increases in cyclic ADP-ribose, $[Ca^{2+}]_i$ and insulin secretion. *J. Biol. Chem. 274*, 1869−1872.

(24) Partida-Sanchez, S., Cockayne, D., Monard, S., Jacobson, E. L., Oppenheimer, N., Garvy, B., Kusser, K., Goodricj, S., Howard, M., Harmsen, A., Randall, T., and Lund, F. E. (2001) Cyclic ADP-ribose production by CD38 regulates intracellular calcium release, extracellular calcium influx and chemotaxis in neutrophils and is required for bacterial clearance in vivo. *Nat. Med. 7*, 1209−1216.

(25) Jin, D., Liu, H. X., Hirai, H., Torashima, T., Nagai, T., Lopatina, O., Shnayder, N. A., Yamada, K., Noda, M., Seike, T., Fujita, K., Takasawa, S., Yokoyama, S., Koizumi, K., Shiraishi, Y., Tanaka, S., Hashii, M., Yoshihara, T., Higashida, K., Islam, M. S., Yamada, N., Hayashi, K., Noguchi, N., Kato, I., Okamoto, H., Matsushima, A., Salmina, A., Munesue, T., Shimizu, N., Mochida, S., Asano, M., and Higashida, H. (2007) CD38 is critical for social behaviour by regulating oxytocin secretion. *Nature 446*, 41−45.

(26) Liu, Q., Graeff, R., Kriksunov, I. A., Jiang, H., Zhang, B., Oppenheimer, N., Lin, H., Potter, B. V., Lee, H. C., and Hao, Q. (2009) Structural basis for enzymatic evolution from a dedicated ADP-ribosyl cyclase to a multi- functional NAD hydrolase. *J. Biol. Chem. 284*, 27637−27645.

(27) Liu, Q., Kriksunov, I. A., Jiang, H., Graeff, R., Lin, H., Lee, H. C., and Hao, Q. (2008) Covalent and noncovalent intermediates of an NAD utilizing enzyme, human CD38. *Chem. Biol. 15*, 1068−1078.

(28) Sauve, A. A., and Schramm, V. L. (2002) Mechanism-based inhibitors of CD38: A mammalian cyclic ADP-ribose synthetase. *Biochemistry 41*, 8455−8463.

(29) Graeff, R. M., Walseth, T. F., Fryxell, K., Branton, W. D., and Lee, H. C. (1994) Enzymatic synthesis and characterizations of cyclic GDP-ribose. A procedure for distinguishing enzymes with ADP-ribosyl cyclase activity. *J. Biol. Chem. 269*, 30260−30267.

(30) Anderson, B. G., Bauta, W. E., Cantrell, W. R. Jr., Engles, T., and Lovett, D. P. (2008) Isolation, Synthesis, and Characterization of Impurities and Degradants from the Clofarabine Process. *Org. Process Res. Dev. 12*, 1229−1237.

(31) Yoshikawa, M., Kato, T., and Takenishi, T. (1969) Studies of phosphorylation. III. Selective phosphorylation of unprotected nucleosides. *Bull. Chem. Soc. Jpn. 42*, 3505−3508.

(32) Puech, F., Gosselin, G., and Imbac, J.-L. (1989) Synthesis of 9-(3-deoxy- and 2,3-dideoxy-3-fluoro-β-D-xylofuranosyl)guanines as potential antiviral agents. *Tetrahedron Lett. 30*, 3171−3174.
(33) Mikhailopulo, I. A., Sivets, G. G., Poopeiko, N. E., and Khripach, N. B. (1995) Oxydation-reduction sequence for the synthesis of peracylated fluorodeoxy pentofuranosides. *Carbohydr. Res. 278*, 71−89.
(34) Graeff, R., and Lee, H. C. (2002) A novel cycling assay for cellular cyclic ADP-ribose with nanomolar sensitivity. *Biochem. J. 361*, 379−384.
(35) Otwinowski, Z., and Minor, W. (1997) Processing of X-ray diffraction data collected in oscillation mode. *Methods Enzymol. 276*, 307−325.
(36) McCoy, A., Grosse-Kunstleve, R., Adams, P., Winn, M., Storoni, L., and Read, R. (2007) Phaser crystallographic software. *J. Appl. Crystallogr. 40*, 658−674.
(37) Collaborative Computational Project Number 4 (1994) The CCP4 Suite: Programs for protein crystallography. *Acta Crystallogr. D50*, 760−763.
(38) Murshudov, G., Vagin, A., and Dodson, E. (1997) Refinement of macromolecular structures by the maximum-likelihood method. *Acta Crystallogr. D53*, 240−255.
(39) Murshudov, G., Vagin, A., and Dodson, E. (1997) Refinement of macromolecular structures by the maximum-likelihood method. *Acta Crystallogr. D53*, 240−255.
(40) Schuttelkopf, A., and Van Aalten, D. (2004) PRODRG: A tool for high-throughput crystallography of protein-ligand complexes. *Acta Crystallogr. D60*, 1355−1363.
(41) Painter, J., and Merritt, E. (2006) TLSMD web server for the generation of multi-group TLS models. *J. Appl. Crystallogr. 39*, 109−111.
(42) Davis, I., Leaver-Fay, A., Chen, V., Block, J., Kapral, G., Wang, X., Murray, L., Bryan Arendall, W. III, Snoeyink, J., and Richardson, J. (2007) MolProbity: All-atom contacts and structure validation for proteins and nucleic acids. *Nucleic Acids Res. 35*, W375−W383.
(43) Munshi, C. B., Graeff, R., and Lee, H. C. (2002) Evidence for a causal role of CD38 expression in granulocytic differentiation of human HL-60 cells. *J. Biol. Chem. 277*, 49453−49458.
(44) Adebanjo, O. A., Anandatheerthavarada, H. K., Koval, A. P., Moonga, B. S., Biswas, G., Sun, L., Sodam, B. R., Bevis, P. J. R., Huang, C. L. H., Epstein, S., Lai, F. A., Avadhani, N. G., and Zaidi, M. (1999) A new function for CD38/ADP-ribosyl cyclase in nuclear Ca^{2+} homeostasis. *Nat. Cell Biol. 1*, 409−414.
(45) Khoo, K. M., Han, M.-K., Park, J. B., Chae, S. W., Kim, U.-H., Lee, H. C., Bay, B. H., and Chang, C. F. (2000) Localization of the cyclic ADP-ribose-dependent calcium signaling pathway in hepatocyte nucleus. *J. Biol. Chem. 275*, 24807−24817.
(46) Gromada, J., Jorgensen, T. D., and Dissing, S. (1995) The release of intracellular Ca^{2+} in lacrimal acinar cells by α,β-adrenergic and muscarinic cholinergic stimulation: The roles of inositol triphosphate and cyclic ADP-ribose. *Pfluegers Arch. 429*, 751−761.
(47) Mitsui-Saito, M., Kato, I., Takasawa, S., Okamoto, H., and Yanagisawa, T. (2003) CD38 gene disruption inhibits the contraction induced by α-adrenoceptor stimulation in mouse aorta. *J. Vet. Med. Sci. 65*, 1325−1330.
(48) Sethi, J. K., Empson, R. M., and Galione, A. (1996) Nicotinamide inhibits cyclic ADP-ribose-mediated calcium signalling in sea urchin eggs. *Biochem. J. 319*, 613−617.
(49) Chen, Z., Kwong, A. K. Y., Yang, Z.-J., Zhang, L. R., Lee, H. C., and Zhang, L. H. (2011) Studies on the synthesis of nicotinamide nucleoside and nucleotide analogues and their inhibitions towards CD38 NADase. *Heterocycles 83*, 2837−2850.